# Thermal and Morphology Properties of Various Silica Contents in Sulfone Epoxy Nanocomposites

**Yie-Chan Chiu,[1] Hsieh-Chih Tsai,[2] Toyoko Imae[2,3]**

[1]*Plating Technology Development Department, Chipbond Technology Corporation, HsinChu, Taiwan 30078, Republic of China*
[2]*Graduate Institute of Applied Science and Technology, National Taiwan University of Science and Technology, Taipei, Taiwan 10607, Republic of China*
[3]*Department of Chemical Engineering, National Taiwan University of Science and Technology, Taipei, 10607 Taiwan, Republic of China*

Received 10 March 2011; accepted 2 October 2011
DOI 10.1002/app.36277
Published online 1 February 2012 in Wiley Online Library (wileyonlinelibrary.com).

**ABSTRACT:** The effect of spherical silica oxide, tetraethoxyl silane (TEOS), and 5 polysilsesquioxane (POSS) derivative on the thermal and morphology properties in the sulfone epoxy (SEP) nanocomposite have been investigated in this study. The hydroxyl group (silanol groups) of silica improved the curing reactivity of SEP and increased the glass transition temperature ($T_g$) from 132°C to 162°C. The POSS type silica formed bulky side-chains in the nanocomposites, and the organic *i*-butyl, ethyl, methyl, and un-reacted hydroxy groups influenced thermal stability. The char yield increased from 35.77% to 42.18% and 1.12% to 7.17% under nitrogen and air in thermal gravimetric analysis, respectively. From an investigation of thermal degradation, it was determined that the introduction of diphenylphosphine modified polysilsesquioxane (DPPP-PSQ), spherical silica particles ($SiO_2$), and TEOS to the SEP enhanced the thermal stability beyond that provided by POSS side-chain SEP nanocomposites. The addition of silica segments provided not only thermally stable char to reduce anti-thermal oxidation properties but also enhanced thermal degradation stability of various silica-containing/SEP nanocomposites. © 2012 Wiley Periodicals, Inc. J Appl Polym Sci 125: E523–E531, 2012

**Key words:** nanocomposite; silica nano particles; epoxy

## INTRODUCTION

Recently, a wide variety of nanocomposite fillers, such as silica,[1] carbon nanotubes,[2] titania,[3] and montmorillonite[4] have been investigated. The unique reinforcing characteristics of nano-sized inorganic fillers are far more effective than developed fillers of other sizes. Organic–inorganic nanocomposites exhibit superior optical properties,[5] mechanical properties,[6] and thermal stability,[7] all of which could be improved through further engineering. The addition of nano-fillers is a crucial element in the quality of the organic polymer matrix; however, nano-size segments not only reinforce the materials but also cause interactions between the organic and inorganic constituents.[8] Generally, investigation into the performance of nanocomposites involves the introduction of nano-size silica filler to enhance the properties of the materials.[9–13]

Nano-size silica is a well-known filler material, providing a number of benefits. The individual nano-size particles possess several distinctive profiles, such as spherical,[14] cage shaped,[15] and network-like diphenylphosphine modified polysilsesquioxane (DPPP-PSQ),[16] and nano-silica composites have found their way into applications such as adhesives, industrial coatings, and the matrices of electronic and electrical equipment.

Most epoxy resins suffer from one significant shortcoming limiting their applicability, thermal stability.[17–20] Promoting thermal stability while reducing the production of harmful waste products in the fabrication process has led to the investigation of many environmentally friendly materials. These novel materials include silica-containing[21,22] and phosphorus-containing[23,24] epoxies. Previous investigations have indicated that the introduction of nano-silica into an organic polymer material can enhance thermal stability.[25–27] Liu et al. and Hsiue et al. indicated that the introduction of silica compounds could increase thermal stability while decreasing adverse environmental effects.[7,19,24,25]

*Correspondence to:* H.-C. Tsai (h.c.tsai@mail.ntust.edu.tw).
Contract grant sponsor: National Science Council of the Republic of China; contract grant number: NSC 100-2221-E-011-030-MY3.
Contract grant sponsor: National Taiwan University of Science and Technology; contract grant number: 100H451201.

The sulfone epoxy (SEP) monomer has been prepared by the method proposed in a previous investigation.[28] In this research, various nano-silica fillers were introduced to the SEP for the preparation of silica-containing/SEP nanocomposites. The morphology and size of the inorganic-silica particles were investigated using transmission electron microscopy (TEM), and the effects of various forms of silica on the thermal properties were also examined. The glass transition temperature ($T_g$) was determined using differential scanning calorimetry (DSC), and the properties of thermal degradation of various silica-containing/SEP nanocomposites were established through thermogravimetric analysis (TGA). Thermal degradation activation energy was calculated according to the Horowitz–Metzger integral method.

## EXPERIMENT

### Materials

SEP[28] and DPPP-PSQ silica compound have been synthesized following the same procedures of previous reports.[11,16] Isocyanatopropyldinethylsilyl-isobutyl-polysilsesquioxane (POSS) (IC) contained seven isobutyl groups and one isocyanate group, with the chemical formula $C_{34}H_{75}NO_{14}Si_9$, and a molar mass of 974.73 g/mol. Glycidyethyl-POSS (EP) contained seven ethyl groups and one epoxy group, with the chemical formula $C_{20}H_{46}O_{14}Si_8$ and a molar mass of 735.25 g/mol. *Trans*-cyclohexanediolisobutyl-POSS (AL1) contained seven cyclohexyl groups and one *trans*-cyclohexanedio group, with a chemical formula of $C_{36}H_{78}O_{14}Si_8$ and a molar mass of 959.68 g/mol. 1,2-Propanediolisobutyl-POSS (AL2) contained seven isobutyl groups and one propanediol group, with a chemical formula of $C_{34}H_{76}O_{15}Si_8$ and a molar mass of 949.64 g/mol. All of the POSS reactants were received from Hybrid Plastics Inc. Fountain Valley, CA. Nano-scale silica oxide particles ($SiO_2$) were obtained from Nissan Chemical Co., Japan. Tetraethoxy silane (TEOS) and 4,4-methylenedianiline (DDM) were purchased from Acros Organic Co., Belgium, and DDM was used as the curing agent. Tetrahydrofuran (THF) was obtained from the Tedia Co. Inc., OH. Scheme 1 illustrates the chemical structure of all the nano-silica fillers used in this study.

### Instrumental methods

The glass transition temperature ($T_g$) was determined using DSC thermograms and recorded with a thermal analyzer DSC-Q10 (Waters Co., MA) at a heating rate of 10 °C/min under nitrogen atmosphere, at a nitrogen gas flow rate of 50 mL/min. Thermal degradation properties were studied using a thermogravimetric analyzer TGA-951 (Waters Co.) at a heating rate of 10 °C/min under nitrogen and air atmospheres, with a gas flow rate of 100 mL/min. A JEOL JEM-1230 TEM was used to analyze the morphology of various silica-containing/SEP nanoconposites using an accelerated voltage of 100 kV. Various silica-containing/SEP nanoconposites were microtomed with a Reichest-Jung ULTRACUTE into 100 nm thick slices in a direction normal to the plane of the film.

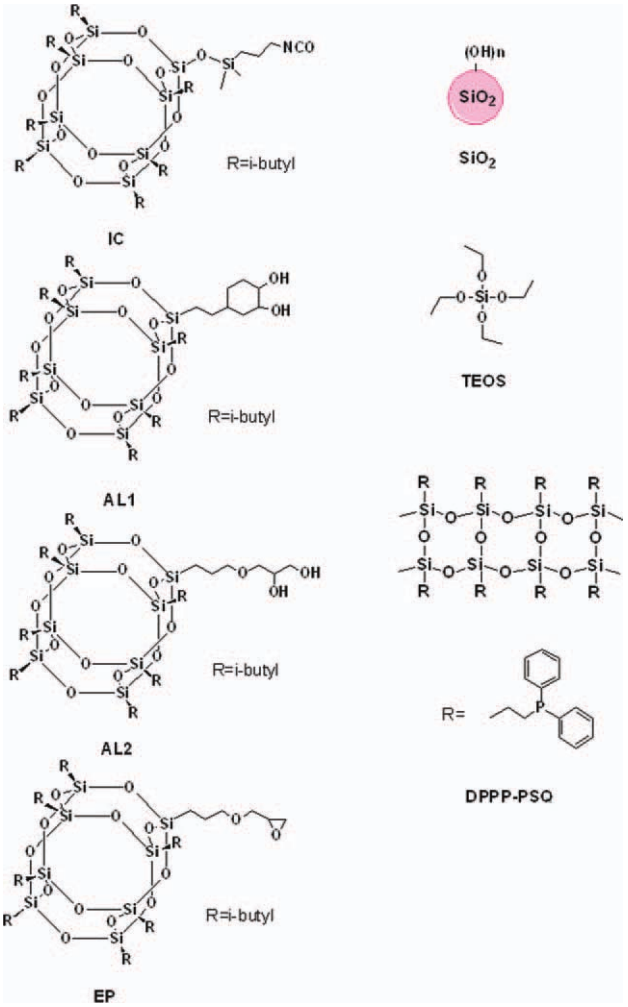


**Scheme 1** Chemical structure of various silica nanoparticles. [Color figure can be viewed in the online issue, which is available at wileyonlinelibrary.com.]

### Preparation of silica-containing/SEP nanocomposites

All of the silica-containing/SEP nanocomposites were prepared at a molar ratio of 2:1.05 for the SEP and DDM curing agent, respectively. The nanocomposites were produced at a 5 wt % weight ratio of various silica fillers to achieve an excellent cross-linking architecture (epoxy weight : silica weight = 100 : 5). The structures of various silica fillers are

displayed in Scheme 1. All of the reactants were homogeneously mixed with the solvent THF at room temperature. The solvent was removed under vacuum at RT (24 h) and further heated to 80°C (2 h), 120°C (2 h), 160°C (4 h), and 180°C (6 h).

### The statistic heat-resistant index ($T_s$)

The statistical heat-resistant index temperature ($T_s$) was determined according to the temperature at which a 5% weight loss ($T_{d5}$) and 30% weight loss ($T_{d30}$) of the sample were observed through TGA. The statistical heat-resistant index temperature ($T_s$) was calculated according to the following equation [eq. (1)][29,30]:

$$T_s = 0.49[T_{d5} + 0.6 \times (T_{d30} - T_{d5})] \quad (1)$$

### The integral procedure decomposition temperature

The integral procedure decomposition temperature (IPDT) was calculated from the method proposed in previous investigations,[31,32] and shown in eq. (2):

$$\mathrm{IPDT}(^{o}\mathrm{C}) = AK(T_f - T_i) + T_i \quad (2)$$

where $A$ is the area ratio of the total experimental curve, defined by the total TGA thermogram traces. $T_i$ and $T_f$ represent the initial temperature and the final temperature, respectively. In this study, the $T_i$ and $T_f$ were 50°C and 800°C, respectively. $A$ and $K$ are calculated using eqs. (3) and (4). The values of $S_1$, $S_2$, and $S_3$ were determined in previous studies.[31,32]

$$A = \frac{S_1 + S_2}{S_1 + S_2 + S_3} \quad (3)$$

$$K = \frac{S_1 + S_2}{S_1} \quad (4)$$

The activation energy of thermal decomposition ($E_a$).[31–33]

The activation energy associated with thermal decomposition was obtained from TGA decomposed traces and calculated according to the Horowitz–Metzger integral method using eq. (5).

$$\ln[\ln(1-\alpha)^{-1}] = \frac{E_a \times \theta}{R \times T_{\max}^2} \quad (5)$$

In eq. (5), $E_a$ is the activation energy of the thermal decomposition, and $\alpha$ is the fraction of thermal decomposition. $T_{\max}$ is defined as the temperature at the maximum rate of weight loss due to thermal decomposition. $\theta$ and $R$ are the $T - T_{\max}$ values and gas constant, respectively. Furthermore, $E_a$ is determined from the slope of the straight line corresponding to the plot of $\ln\{\ln(1-\alpha)^{-1}\}$ versus $\theta$.

## RESULTS AND DISCUSSION

### The morphology of silica-containing/SEP nanocomposites

Figure 1 is a TEM image of various silica-containing/SEP nanocomposites. The black dots represent inorganic silica particles (inorganic segment), with a particle size smaller than 25 nm (the scale bar represents 50 nm). Small silica particle size was obtained in EP, AL1, and AL2 nanpcomposite and the size is around 10 nm. For IC, DPPP-PSQ, TEOS, and $SiO_2$ nanocomposite, the large size of silica particle around 25 nm was found in TEM results. Homogeneous dispersions of silica particles were found in POSS derivative(IC, AL1, AL2, and EP)/SEP nanocomposite when compared with TEOS/SEP and $SiO_2$/SEP. It might due to the site isolation effect of the bulky POSS silica derivative such as AL1, AL2, EP, and IC, which could avoid the aggregation of silica particle in bulk materials when compared with TEOS and $SiO_2$. Therefore, the particles size for AL1, AL1, EP, and IC were 10 nm in the SEP nanocompsoite, In addition, TEM microphotography failed to reveal any phase separation, indicating that the various silica-containing/SEP nanocomposites exhibited good miscibility between organic and inorganic phases.

### Glass transition temperature of silica-containing/SEP nanocomposites

Glass transition temperature ($T_g$) of silica-containing/SEP nanocomposite was determined through DSC analysis. Table I presents the $T_g$ of various silica-containing/SEP nanocomposites, with $T_g$ values in the range of 107–178°. The $T_g$ of 5-IC, 5-AL1, and 5-AL2 were 112°C, 130°C, and 122°C, respectively. These values were lower than those of pristine cured SEP/DDM (132°C). The bulky POSS side-chain might decrease the reactivity of curing and enhance the generation of oligomers. Additionally, bulky side-chains could improve the mobility of the polymer chain and increase the free volume. IC possesses an isocyanate group (NCO group) forming urethane-like side-chain linkages (soft linkage, shown in Scheme 2). Consequently, the $T_g$ of 5-IC/SEP nanocomposite is lower than other silica-containing /SEP nanocomposites. AL1 and AL2 possess two hydroxyl groups, serving as curing agents. The hydroxyl groups could cure the SEP and inhibit a decrease in $T_g$. Consequently, 5-AL1 and 5-AL2 fillers are better choices than 5-IC filler with regard to $T_g$. Moreover,

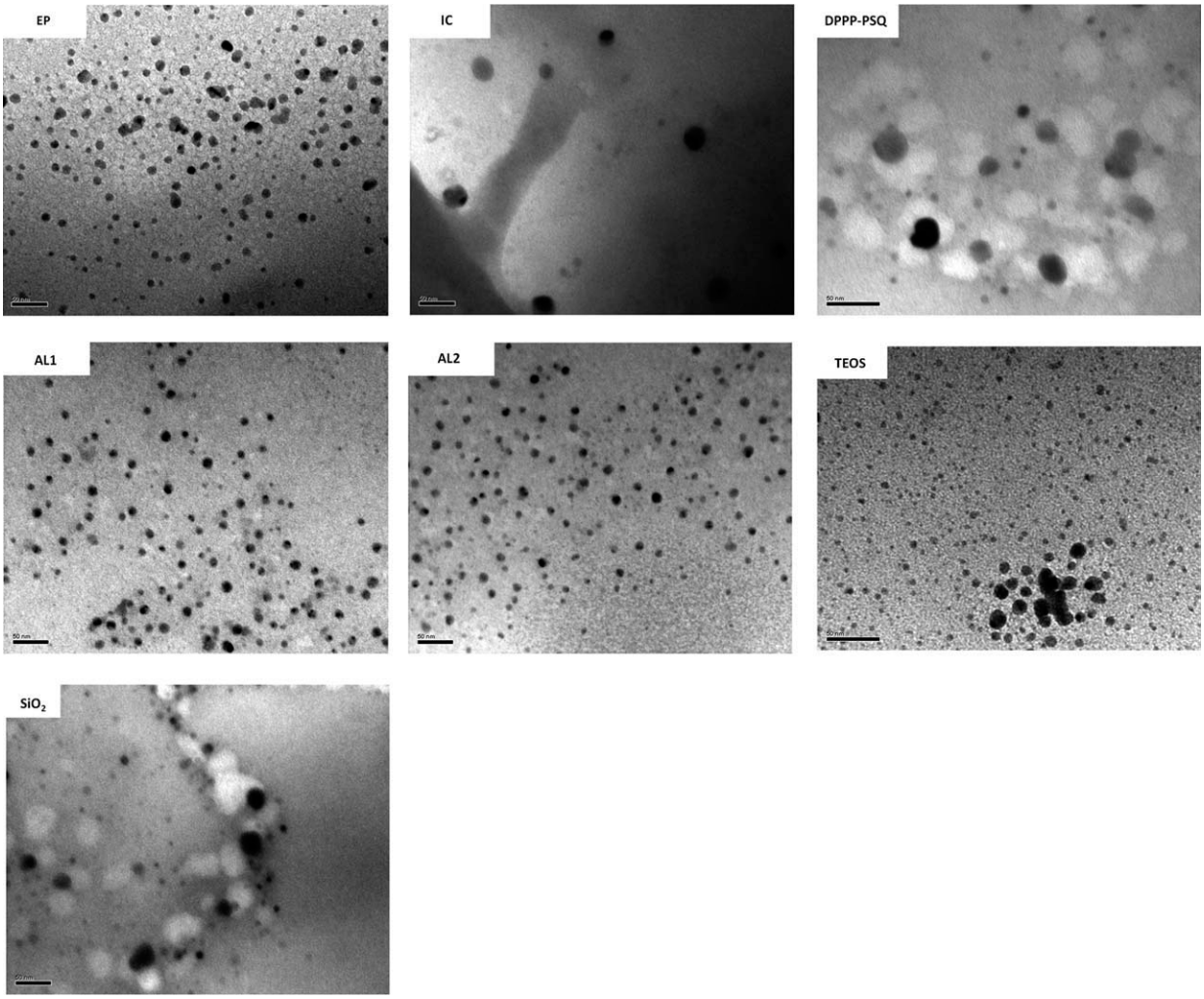


**Figure 1** TEM microphotography of 5-EP, 5-IC, DPPP-PSQ, 5-AL1, 5-AL2, 5-TEOS, and 5-$SiO_2$ nanocomposites.

the lower $T_g$ of 5-AL1 and 5-AL2 occurred in nanocomposite could also be explained from the particle distribution in TEM. Small silica particle embed in the polymer matrix, increasing the spacing and free volume. Therefore, polymer chain could have flexible chain at lower temperature when compared with pristine cured SEP/DDM.

**TABLE I**
**Thermal Properties of Various Silica-Containing/SEP Nanocomposites**

| Sample | $T_g$ | $T_{d5}$[a] | $T_{d5}$[b] | $Char_{800C}$[a] | $Char_{800C}$[b] |
|---|---|---|---|---|---|
| SEP/DDM | 132 | 282 | 281 | 35.77 | 1.12 |
| 5-EP | 146 | 271 | 280 | 39.31 | 2.02 |
| 5-IC | 112 | 207 | 193 | 33.57 | 2.07 |
| 5-AL1 | 130 | 236 | 231 | 36.03 | 2.15 |
| 5-AL2 | 122 | 221 | 199 | 29.76 | 2.09 |
| 5-DPPP-PSQ | 162 | 282 | 279 | 40.19 | 4.57 |
| 5-TEOS | 154 | 289 | 283 | 36.72 | 2.33 |
| 5-$SiO_2$ | 155 | 267 | 257 | 42.18 | 7.17 |

[a] In the nitrogen atmosphere.
[b] In the air atmosphere.

Other nano-silica fillers could be used to enhance the $T_g$. The EP possesses epoxy groups that improve the solubility and curing reactivity associated with the SEP curing reaction. Therefore, the influence of particle size in the $T_g$ was not the main factor for EP, even the particle size is similar with 5AL1 and 5AL2 revealed in TEM results. For this reason, the $T_g$ of 5-EP is higher than that of pristine cured SEP/DDM and other SEP/side-chain POSS nanocomposites. In addition, the nano-effect of the nano-silica fillers improves $T_g$ was also obtained in this study, the $T_g$s of the SEP nanocomposites containing DPPP-PSQ, TEOS, and $SiO_2$ were 162°C, 154°C, and 155°C, respectively. Additionally, the DPPP-PSQ, TEOS, and $SiO_2$ possess numerous hydroxyl groups (silanol groups, Si-OH), which cure with the SEP to improve the cross-linking architecture. Unlike the side-chain POSS fillers, the silanol groups of the DPPP-PSQ type silica, TEOS and $SiO_2$ may connect with the SEP main chain (the chemical structure displayed in Scheme 3). Consequently, the $T_g$ of the DPPP-PSQ, 5-TEOS, and 5-$SiO_2$ are higher than that of SEP/side-chain POSS nanocomposites.

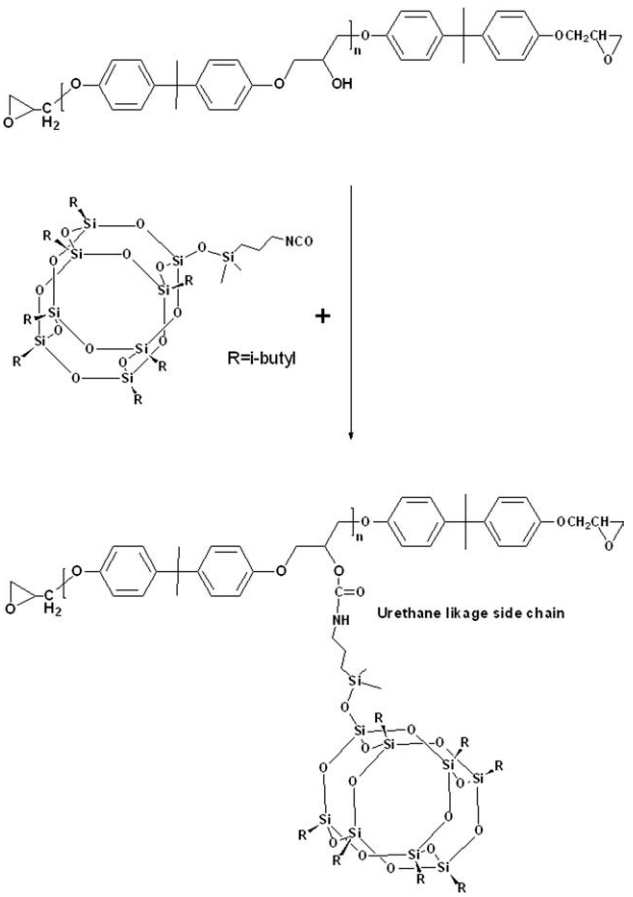


**Scheme 2** Urethane like side chain in 5-IC/SEP nanocomposite.

### Thermal degradation properties of silica-containing/SEP nanocomposites

Figures 2 and 3 illustrate the TGA investigation under nitrogen and air atmospheres, respectively. The properties of thermal degradation are summarized in Tables I and II. The $T_{d5}$ of 5-IC was 206°C, which was lower than that of other silica-containing/SEP nanocomposites. This was due to the fact that 5-IC possesses organic alkyl groups (*i*-butyl groups) and a urethane-like side-chain linkage (as shown in Scheme 2), which are thermally unstable organic groups that could degrade at lower temperatures than other silica-containing/SEP nanocomposites. Moreover, the bulky POSS side-chain and *i*-butyl groups of the POSS could interfere with the SEP curing reaction, resulting in a lower $T_{d5}$ value for 5-IC, 5-AL1, and 5-AL2/SEP nanocomposites than for pristine cured SEP/DDM. The epoxy ring of the EP0417 could be easily cured with DDM (better solubility than other POSS fillers), and the ethyl group of the EP also causes less steric effect than *i*-butyl group in the SEP curing reaction. Tamaki et al.[34] indicated that a lower degree of polymerization reactivity might decrease thermal stability. Consequently, 5-EP exhibited a higher $T_{d5}$ value than other SEP/side-chain POSS nanocomposites did.

For 5-DPPP-PSQ, 5-TEOS, and 5-$SiO_2$ nanocomposites, the chemical structure of the DPPP-PSQ comprised Si and P elements, which could combine to provide a synergistic effect, thereby improving thermal stability.[11,32,35] 5-TEOS forms thermally stable silica segments and disperses homogeneously throughout the SEP matrix, preventing the 5-TEOS nanocomposite from thermal degrading. However, the $T_{d5}$ of 5-$SiO_2$ was lower than that of 5-TEOS, because the $SiO_2$ possesses fewer unreacted hydroxyl groups (silanol groups, Si-OH, shown in Scheme 3), which could decompose at low temperature. Artiaga and coworkers[36] also determined that a small proportion of silanol groups in the silica compounds could negatively influence the silica/epoxy nanocomposites, thereby diminishing the thermal stability of the nanocomposites.

Generally, the char yield of silica-containing/SEP nanocomposites is higher than that of pristine cured SEP/DDM under nitrogen atmosphere. Carbon-based char and inorganic silica char form the components of residue under nitrogen atmosphere. The char yield of 5-IC and 5-AL2 nanocomposites was lower than that of pristine cured SEP/DDM under a nitrogen atmosphere, because 5-IC and 5-AL2 nanocomposites possess urethane-like side-chain linkages, ether linkage (soft linkage), organic *i*-butyl, and methyl groups. Organic functional groups are thermally unstable, decomposing more easily than the sulfone group of SEP,[37] which generates a char yield of thermally stable sulfate derivatives during the process of thermal degradation.[28] The bulky POSS side-chain could generate oligomers in the SEP curing reaction; hence, the char yield of pristine cured SEP/DDM is higher than 5-IC or 5-AL2 nanocomposite.

Under air atmosphere, the entire char yield of the silica-containing/SEP nanocomposites was higher than that of pristine cured SEP/DDM, because the inorganic silica segments were capable of providing

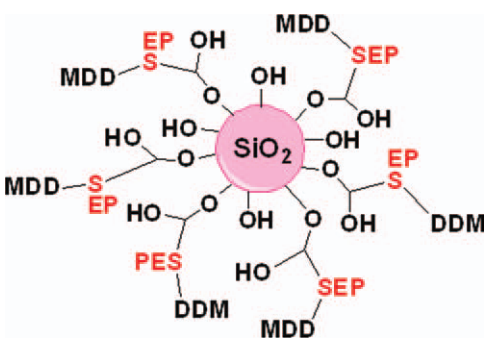


**Scheme 3** Chemical structure of $SiO_2$ cured with SEP. [Color figure can be viewed in the online issue, which is available at wileyonlinelibrary.com.]

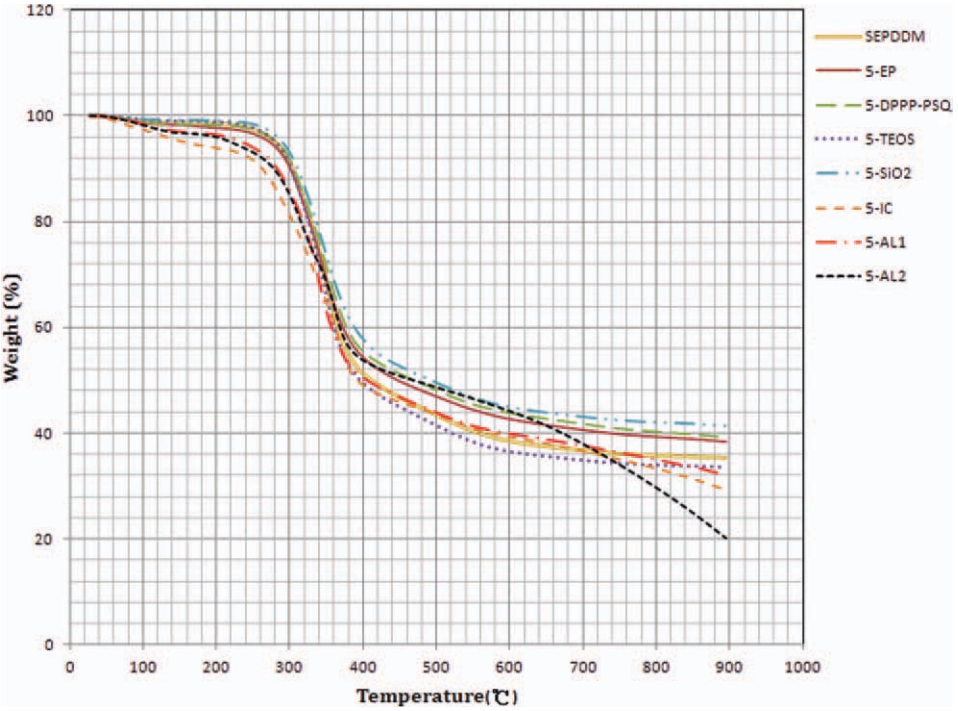


**Figure 2** Thermal degradation trace of various silica-containing/SEP nanocomposites under the nitrogen atmosphere. [Color figure can be viewed in the online issue, which is available at wileyonlinelibrary.com.]

anti-thermal oxidation properties and increasing char yield.[38,39] Liu and coworkers[38] indicated that introduction of the silica segments into the epoxy not only increases the char yield but also improves flame retardancy. Silica possesses low potential surface energy and could migrate to the surface of the cured epoxy material, thereby serving as a thermally stable insulating layer under air atmosphere.[32,35,38] From Table I, 5-DPPP-PSQ and 5-$SiO_2$ nanocomposites possess a higher proportion of residue than other silica-containing/SEP nanocomposites. 5-DPPP-PSQ nanocomposite exhibited good char yield under nitrogen

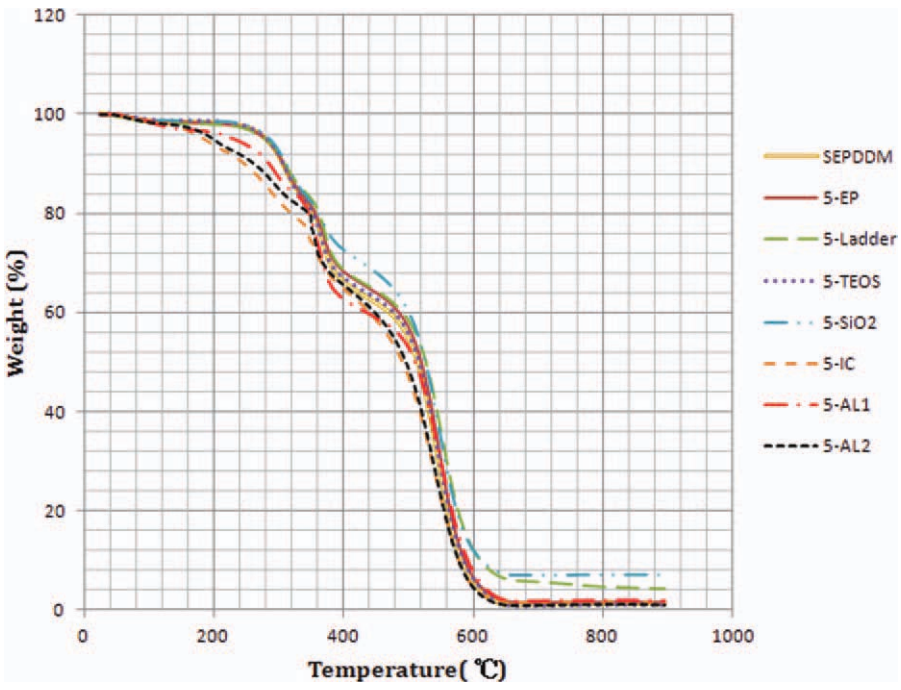


**Figure 3** Thermal degradation trace of various silica-containing/SEP nanocomposites under the air atmosphere. [Color figure can be viewed in the online issue, which is available at wileyonlinelibrary.com.]

**TABLE II**
**Thermal Degradation Parameters of Various Silica-Containing/SEP Nanocomposites**

| Sample | IPDT[b] | IPDT[c] | $E_a$[b] | $E_{a1}$[c] | $E_{a2}$[c] | $T_s$[b] | $T_s$[c] |
|---|---|---|---|---|---|---|---|
| SEP/DDM | 1206.97 | 483.89 | 81.03 | 60.64 | 91.72 | 157.70 | 166.57 |
| 5-EP | 1388.79 | 490.09 | 74.41 | 54.00 | 105.70 | 155.44 | 168.71 |
| 5-IC | 1028.75 | 416.61 | 50.20 | 33.15 | 93.84 | 137.97 | 142.55 |
| 5-AL1 | 1138.06 | 474.32 | 67.20 | 66.20 | 86.54 | 145.69 | 153.34 |
| 5-AL2 | 1127.20 | 460.84 | 54.91 | 32.81 | 87.28 | 145.12 | 147.06 |
| 5-DPPP-PSH | 1359.80 | 528.00 | 72.41 | 51.24 | 97.37 | 159.04 | 169.37 |
| 5-TEOS | 1235.99 | 488.72 | 89.56 | 59.44 | 97.87 | 158.05 | 167.25 |
| 5-$SiO_2$ | 1530.98 | 561.38 | 87.65 | 39.99 | 95.30 | 148.73 | 160.31 |

[a]The unit of the thermal degradation kinetics were kJ/mol and calculated by Horwitz–Metzger equation.
[b] Under the nitrogen atmosphere.
[c] Under the air atmosphere.

and air atmosphere, resulting from phosphorus and silicon elements in the nanocomposite combining to provide a P/Si synergistic effect, thus exhibiting a high degree of efficiency in the formation and preservation of char at high temperatures.[7,32,35] Additionally, phosphorus also could improve the char yield of the polymer.[40] It is possible that the 5-$SiO_2$ nanocomposite produced a greater quantity of residue than 5-DPPP-PSQ nanocomposite, because the silicon char is more thermally stable than phosphorus char at high temperatures.[7] The silanol groups of the $SiO_2$ could serve as curing agents for the SEP, further improving the strength of the cross-linking architecture and the formation of char.[41]

The IPDT values represent the decomposition characteristics related to the volatile composition and thermal degradation properties of the polymer. Generally, introducing silica fillers into a polymer increases the IPDT values, by reducing the volatile fraction of the polymer and improving the thermal degradation stability of the nanocomposite. Consequently, the IPDT values of various silica-containing/SEP nanocomposites are higher than those of pristine cured SEP/DDM. However, the IPDT values of the 5-IC, 5-AL1, and 5-AL2 nanocomposites were lower than those of pristine cured SEP/DDM, because the organic functional groups (*i*-butyl, methyl, and ethyl) of the POSS decompose at a lower temperature than pristine cured SEP/DDM does, thereby increasing the volatile composition (organic segments) of the nanocomposites. The $T_s$ values of 5-IC, 5-AL1, and 5-AL2 were also lower than those of pristine cured SEP/DDM, because the $T_s$ values were determined according to the $T_{d5}$ and $T_{d30}$ values. 5-IC, 5-AL1, and 5-AL2 nanocomposites possess POSS side-chains, which interfere with the curing reaction of epoxy and generate oligomers. The oligomers, urethane-like side-chain linkages (soft linkage), and *i*-butyl and methyl groups decomposed at lower temperatures than the pristine cured SEP/DDM. Consequently, the $T_s$ values of 5-IC, 5-AL1, and 5-AL2 nanocomposites were lower than those of pristine cured SEP/DDM. The $SiO_2$ possesses several unreacted silanol groups, which could decrease the thermal decomposition temperature and $T_s$ value.

Thermal degradation activation energy was calculated according to the Horowitz–Metzger integral method[31–33] under nitrogen and air atmospheres, as summarized in Table II. In the epoxy curing reaction, the POSS type side-chain may have caused the generation of oligomers, and the POSS possessed organic *i*-butyl, ethyl, and methyl groups. Therefore, the thermal degradation activation energy of 5-EP, 5-IC, 5-AL1, and 5-AL2 nanocomposites was lower than that of pristine cured SEP/DDM under nitrogen atmosphere. The thermal degradation activation energy of 5-IC and 5-AL2 nanocomposites was lower than 5-EP or 5-AL1 nanocomposites. Because the 5-IC0655 nanocomposite possessed urethane-like side-chain linkages (soft linkage, shown in Scheme 2), the AL0130 possessed an organic ether group and unreacted hydroxyl groups, which could easily lead to thermal decomposition. For 5-DPPP-PSQ nanocomposite, the phosphorus with the DPPP-PSQ-type silica could decompose at low temperature to form a thermally stable char yield. Consequently, the $E_a$ value of 5-DPPP-PSQ nanocomposite was lower than that of pristine cured SEP/DDM. However, following thermal degradation, the silica could migrate to the surface of the nanocomposite, to serve as a thermally stable layer, preventing the nanocomposite from further thermal degradation. Camino et al.[42] indicated that the thermal decomposition energy of the C—Si bond was 78 kcal/mol, which is lower than that of a Si—O bond (108 kcal/mol). Hence, 5-TEOS and 5-$SiO_2$ nanocomposites could increase the thermal degradation energy.

Under air atmosphere, the activation energy in the first stage of thermal degradation ($E_a$1s) of 5-TEOS and 5-$SiO_2$ nanocomposites was lower than that of pristine cured SEP/DDM, because the silicon segments protected the char.[32] The silica segments decompose easily to form a thermally stable char

yield, providing anti-thermal oxidation properties in the second stage of thermal degradation under air atmosphere. Consequently, the activation energy in the second stage of thermal degradation ($E_a$2s) of 5-TEOS and 5-$SiO_2$ nanocomposites was higher than that of pristine cured SEP/DDM. For the 5-DPPP-PSQ nanocomposite, the $E_a$2 was also higher than that of pristine cured SEP/DDM; however, the $E_a$1 was lower. The phosphorus segments decomposed at a lower temperature than the pristine cured SEP/DDM did, forming thermally stable char. Meanwhile, the silica segments degraded and migrated to the surface of the nanocomposite, wherein it served as a thermally stable layer under air atmosphere. The $E_a$2 of 5-EP and 5-IC nanocomposites was higher than that of pristine cured SEP/DDM. However, the $E_a$1 of 5-EP and 5-IC nanocomposites was lower than that of pristine cured SEP/DDM. The thermal degradation of the organic *i*-butyl, ethyl, and urethane-like side-chain linkages (soft linkage, see Scheme 2) was induced in the first stage of thermal degradation under air atmosphere. The IC0655 architecture possesses a structure of Si—$CH_3$, which could degrade easily in the first stage of thermal degradation to generate a thermally stable char under air, which could prevent the thermal decomposition of the nanocomposite. The epoxy ring of the EP0417 improves miscibility in the SEP curing reaction, thereby improving curing reactivity and the degree of cross-linking. Consequently, the $E_a$2 of 5-EP and 5-IC nanocomposites was higher than the $E_a$1. Nonetheless, the $E_a$1 of 5-AL1 nanocomposite was higher than that of other silica-containing/SEP nanocomposites, because the AL1 possesses a cyclic hexane group, which resists decomposition in the first stage of thermal degradation under air. The $E_a$1 of 5-AL2 nanocomposite was lower than that of other silica-containing/SEP nanocomposites, because the AL2 possesses an aliphatic ether group, which is a soft functional group, susceptible to decomposition in the first stage of thermal degradation under air. Consequently, the architecture and curing reactivity of nano-silica plays a crucial role in improving thermal stability.

## CONCLUSION

This study introduced various silica fillers into the SEP material, for the preparation of silica-containing/SEP nanocomposites. All of the silica segments in the various silica-containing/SEP nanocomposites exhibited good miscibility between organic and inorganic phases, with no evidence of phase separation. The particle size of the silica segments was less than 25 nm. The DPPP-PSQ type silica, TEOS, and $SiO_2$ possessed numerous hydroxyl groups (silanol groups), capable of curing with the epoxy group of the SEP, to improve the glass transition temperature ($T_g$) from 132 to 154°C. From an investigation of thermal degradation, it was found that various silica segments might decompose and migrate to the surface of the nanocomposite to serve as a thermally stable layer, thereby enhancing anti-thermal oxidation properties. Additionally, the DPPP-PSQ-type silica, TEOS, and $SiO_2$ nanocomposites possessed superior thermal stability over those of the SEP/side-chain POSS nanocomposites. The char yield of the various silica-containing/SEP nanocomposites increased from 35.77 to 42.18 and 1.12 to 7.17, leading to an improvement in IPDT values from 1206.97 to 1530.98 and 483.89 to 561.38 under nitrogen and air atmospheres, respectively. Under air atmosphere, the thermal degradation activation energy improved from 91.72 kJ/mol to 105.7 kJ/mol.

## References


1. He, J. P.; Li, H. M.; Wang, X. Y.; Gao, Y. Eur Polym J 2006, 42, 1128.
2. Wu, H. L.; Yang, Y. T.; Ma, C. C. M.; Kuan, H. C. J Polym Sci Part A: Polym Chem 2005, 43, 6084.
3. Perrin, F. X.; Nguyen, V. N.; Vernet, J. L. Macromol Chem Phys 2005, 206, 1439.
4. Mailhot, B.; Morlat-Thérias, S.; Bussiére, P. O.; Pluart, L. L.; Duchet, J.; Sautereau, H.; Gérard, J. F.; Gardette, J. L. Polym Degrad Stab 2008, 93, 1786.
5. Asuka, K.; Liu, B.; Terano, M.; Nitta, K. Macromol Rapid Commun 2006, 27, 910.
6. Lu, H.; Shen, H.; Song, Z.; Shing, K. S.; Tao, W.; Nutt, S. Macromol Rapid Commun 2005, 26, 1445.
7. Hsiue, G. H.; Liu, Y. L.; Tsiao, J. J Appl Polym Sci 2000, 78, 1.
8. Boutti, S.; Bourgeat-Lami, E.; Zydowicz, N. Macromol Rapid Commun 2005, 26, 1860.
9. Wang, L. F.; Ji, Q.; Glass, T. E.; Ward, T. C.; McGrath, J. E.; Muggli, M.; Burns, G.; Sorathia, U. Polymer 2000, 41, 5083.
10. Ho, T. H.; Wang, C. S. Eur Polym J 2001, 37, 267.
11. Chiu, Y. C.; Ma, C. C. M.; Liu, F. Y.; Chiang, C. L.; Riang, L.; Yang, J. C. Eur Polym J 2008, 44, 1003.
12. Lin, S. T.; Huang, S. K. J Polym Sci Part A: Polym Chem 1996, 34, 869.
13. Liu, Y. L.; Yu, C. H.; Lee, K. R.; Lai, J. Y. J Membr Sci 2007, 287, 230.
14. Liu, Y. L.; Hsu, C. Y.; Su, Y. H.; Lai, J. Y. Biomacromolecules 2005, 6, 368.
15. Matejka, L.; Strachota, A.; Pleštil, J.; Whelan, P.; Steinhart, M.; Šlouf, M. Macromolecules 2004, 37, 9449.
16. Chiang, C. L.; Ma, C. C. M. J Polym Sci Part A: Polym Chem 2003, 41, 1371.
17. Spontón, M.; Ronda, J. C.; Galiá, M.; Cádiz, V. J Polym Sci Part A: Polym Chem 2007, 45, 2142.
18. Lu, G.; Huang, Y.; Yan, Y.; Zhao, T.; Yu, Y. J Polym Sci Part A: Polym Chem 2003, 41, 2599.
19. Chiang, C. L.; Ma, C. C. M. Polym Degrad Stab 2004, 83, 207.
20. Wu, C. S.; Liu, Y. L. J Polym Sci Part A: Polym Chem 2004, 42, 1868.
21. Liu, Y. L.; Chiu, Y. C.; Wu, C. S. J Appl Polym Sci 2003, 87, 404.
22. Hsiue, G. H.; Wang, W. J.; Chang, F. C. J Appl Polym Sci 1999, 73, 1231.
23. Lin, J. F.; Ho, C. F.; Huang, S. K. Polym Degrad Stab 2000, 67, 137.

24. Wang, T. S.; Parng, J. K.; Shau, M. D. J Appl Polym Sci 1999, 74, 413.
25. Wang, C. S.; Shieh, J. Y. Eur Polym J 2000, 36, 443.
26. Espinosa, M. A.; Cádiz, V.; Galiá, M. J Polym Sci Part A: Polym Chem 2004, 42, 279.
27. Canadell, J.; Mantecón, A.; Cádiz, V. J Polym Sci Part A: Polym Chem 2007, 45, 1980.
28. Chiu, Y. C.; Chou, I. C.; Tseng, W. C.; Ma, C. C. M. Polym Degrad Stab 2008, 93, 668.
29. Jiang, B.; Hao, J.; Wang, W.; Jiang, L.; Cai, X. Eur Polym J 2001, 37, 463.
30. Grimbley, M. R.; Lehrle, R. S. Polym Degrad Stab 1995, 49, 223.
31. Park, S. J.; Cho, M. S. J Mater Sci 2000, 35, 3525.
32. Wu, C. S.; Liu, Y. L.; Chiu, Y. C.; Chiu, Y. S. Polym Degrad Stab 2002, 78, 41.
33. Doyle, C. D. Anal Chem 1961, 33, 77.
34. Tamaki, R.; Choi, J.; Laine, R. M. Chem Mater 2003, 15, 793.
35. Liu, Y. L.; Chou, C. I. Polym Degrad Stab 2005, 90, 515.
36. Tarrío-Saavedra, J.; López-Beceiro, J.; Naya, S.; Artiaga, R. Polym Degrad Stab 2008, 93, 2133.
37. Liu, Y. L.; Lee, H. C. J Polym Sci Part A: Polym Chem 2006, 44, 4632.
38. Hsiue, G. H.; Liu, Y. L.; Liao, H. H. J Polym Sci Part A: Polym Chem 2001, 39, 986.
39. Liu, Y. L.; Hsu, C. Y.; Hsu, K. Y. Polymer 2005, 46, 1851.
40. Liu, Y. L.; Chiu, Y. C. J Polym Sci Part A: Polym Chem 2003, 41, 1107.
41. Liu, Y. L.; Li, S. H. J Appl Polym Sci 2005, 95, 1237.
42. Camino, G.; Lomakin, S. M.; Lazzari, M. Polymer 2001, 42, 2395.